2006-01-1085

Air Path Estimation on Diesel HCCI Engine

J. Chauvin, N. Petit, P. Rouchon
École des Mines de Paris

G. Corde
IFP

C. Vigild
Ford Forschungszentrum Aachen GmbH

ABSTRACT

In this paper, we address the problem of air path variables estimation for an HCCI engine. Two observers are proposed. Both rely on physical assumptions on the combustion, but use different sensors. After proving convergence in the two cases, we carry out comparisons based on simulation results. We stress the impact of two particular additional sensors on obtained performance: fresh air and EGR temperature probes.

INTRODUCTION

Increasingly stringent pollution standards norms have spurred a broad interest in the reduction of global engine emissions. Lately, two strategies have emerged: after-treatment and direct combustion emissions reduction. For Diesel engines, equipments required by after-treatment and implementation issues usually carry high cost premiums. An alternative is to use a cleaner combustion mode. Therefore, the Highly Premixed Combustion mode (HPC) – including Homogeneous Charge Compression Ignition (HCCI) – has become of major interest in recent years. It requires the use of high Exhaust Gas Recirculation (EGR) rates. The key idea is that the inert burned gas in the cylinder lower the temperature and dilute the air charge which reduce the emissions of nitrogen oxides. In practice, numerous experimentations brought the proof of significant emission reduction (see [1, 2, 3] for example). Yet, actual vehicle implementation implies frequent transients which reveal to be much more complex than steady state experimentation.

The HCCI combustion mode consists of preparing a highly diluted burned gas/air/fuel mixture. Simultaneous ignition in the whole combustion chamber is performed and controlled. In that mode, the Burned Gas Rate (BGR $\triangleq 1 - \frac{M_{int,air}}{M_{int}}$), which is the mass of burned gas over the total mass in the intake manifold, plays a key role. Notice that the BGR is different of the EGR due to the presence of air in the EGR (lean combustion). Offsets on BGR may cause misfires and additive noises. In the HCCI combustion mode, BGR has a very high value (40% or more). Accurate control of BGR can be achieved by controlling the airpath system: intake and exhaust manifolds, EGR loop and VGT. Unfortunately, until now, the use of a gas composition sensor (like the AFR sensor) in the intake manifold seems out of reach for commercial engines. In facts, temperature is too low for the sensor. Observers are thus needed. Some have already been presented (see [4], [5] for example). The contribution of this paper is the design of two original BGR observers. Both are validated theoretically and in simulation. The first one is based on masses balance and an isothermal assumption (variations of the temperature in the intake manifold are assumed very small). The second one considers an additional energy balance in the reference system. Accurate EGR and aspirated flows estimation is done with two additional temperature sensors (fresh air and EGR temperatures). In both cases, the proposed technique relies only on commercial-line engine sensors. In the adiabatic case, the static error on aspirated flow is eliminated and leads to the convergence of both the EGR flow and the BGR. Performance are evaluated bearing on my mind our long term goal: active control of the BGR in the intake manifold.

The paper is organized as follows. In Section 2, we present the model of the intake manifold. A first observer corresponding to the isothermal case is presented in Section 3. The adiabatic case is studied in Section 4. The simulation set up is detailed in Section 5. Simulation results are reported in Section 6. Finally, conclusions and future directions are detailed in Section 7.

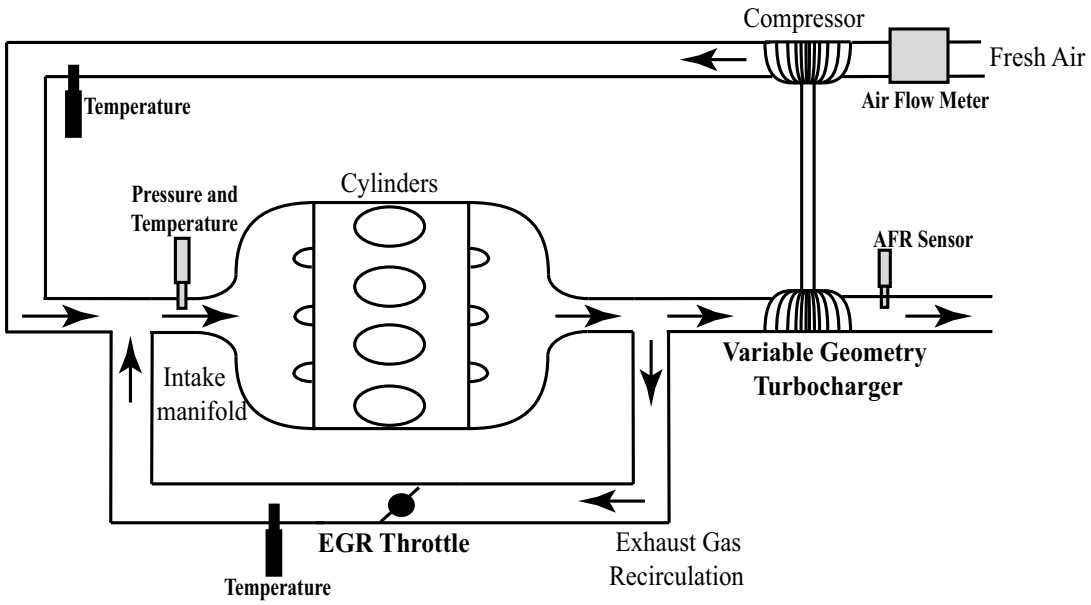

Figure 1: Air Charge Estimation problem. The grey sensors (pressure and temperature in the intake manifold, AFR sensor located downstream the turbine, and air flow meter) are the sensors used for our isothermal observer. The black sensors (fresh air and EGR temperature probes) are added for our adiabatic observer.

INTAKE MANIFOLD MODELLING

Figure 1 shows the flow sheet of the burned gas rate estimation problem. Flows from the fresh air (measured by the Manifold Air Flow) and the Exhaust Gas Recirculation (EGR) come into the intake manifold and are aspirated into the cylinders. We use mass balances, ideal gas law, and consider a low time resolution (180^o TDC time scale). In particular, high frequency aspiration phenomena are not taken into account. A nomenclature is presented in Table 1.

MASS BALANCE IN THE INTAKE MANIFOLD Ideal gas law leads to

$$P_{int}V_{int} = M_{int}RT_{int}$$

The mass balance writes

$$\dot{P}_{int} = \frac{R}{V_{int}}(\gamma_{air}D_{air}T_{air} + \gamma_{egr}D_{egr}T_{egr} - \gamma_{int}D_{asp}T_{int}) \tag{1}$$

Classically (see [6] for exemple), we define the aspirated flow as

$$D_{asp} = \eta_{vol}(P_{int}, N_e)\frac{P_{int}}{RT_{int}}V_{cyl}\frac{N_e}{120} \tag{2}$$

where V_{cyl} is the cylinder volume. η_{vol} is the volumetric efficiency which is experimentally derived and, eventually, defined though a look-up table $\eta_{vol,map}(P_{int}, N_e)$ as presented in Figure 2. Values vary with engine operating conditions (mainly intake pressure and engine speed). At first order, we note

$$\eta_{vol}(P_{int}, N_e) = \eta_{vol,map}(P_{int}, N_e) + \delta\eta$$

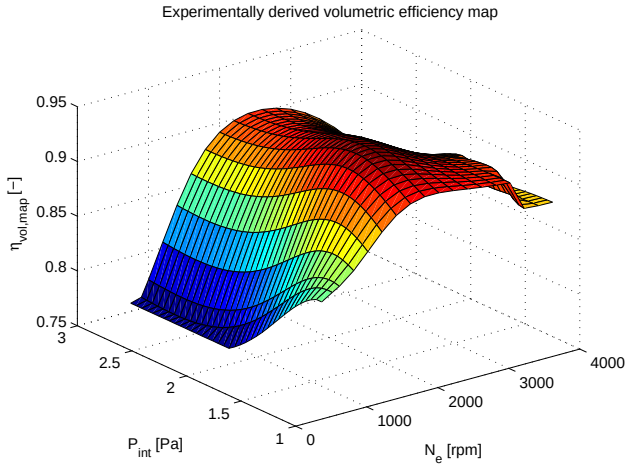

Figure 2: Experimentally derived volumetric efficiency map at steady state.

The energy balance yields

$$\begin{aligned}\dot{T}_{int} &= \frac{R}{V_{int}P_{int}}\big(D_{air}(\gamma_{air}T_{air} - T_{int}) \\ &\quad -D_{asp}(\gamma_{int} - 1)T_{int} + D_{egr}(\gamma_{egr}T_{egr} - T_{int})\big)\end{aligned} \tag{3}$$

The burned gas ratio F_{int} is the fraction of air in the intake manifold. It writes

$$F_{int} \triangleq 1 - \frac{M_{int,air}}{M_{int}}$$

Composition of the EGR (F_{exh}) is measured by the Air Fuel Ratio sensor located downstream the turbine. Mixing dynamics is modelled as

$$\dot{F}_{int} = \frac{RT_{int}}{P_{int}V_{int}}(D_{egr}(F_{exh} - F_{int}) - D_{air}F_{int}) \tag{4}$$

Table 1: Nomenclature. i.m. and e.m refer to the intake and exhaust manifold repesctively.

Symb.	Quantity	Unit
P_{int}	Pressure in the i.m.	Pa
T_{int}	Temperature in the i.m.	K
M_{int}	Total mass in the i.m.	kg
$M_{int,air}$	Air mass in the i.m.	kg
V_{int}	i.m. volume	L
N_e	Engine Speed	rpm
D_{air}	Manifold air flow	kg.s^{-1}
D_{egr}	EGR flow	kg.s^{-1}
D_{asp}	Flow aspirated into the cylinders	kg.s^{-1}
V_{cyl}	Cylinders volume	L
T_{air}	Fresh air temperature	K
T_{egr}	EGR temperature	K
γ_{air}	Specific heats ratio (fresh air)	-
γ_{egr}	Specific heats ratio (EGR)	-
γ_{int}	Specific heats ratio (i.m.)	-
F_{int}	Burned gas fraction in the i.m.	-
F_{exh}	Burned gas fraction in the e.m.	-
R	Ideal gas constant	J.(kgK)$^{-1}$
η_{vol}	Volumetric efficiency	-
$\eta_{vol,map}$	Experimental volumetric efficiency at steady state	-
$\delta\eta$	Volumetric efficiency error	-
u	EGR valve normalized effective area	-

We note

$$D_{\text{egr}} = g(u)$$

where g is a strictly increasing function of the EGR valve effective area u (known by measurement of the position of the EGR valve) with $g(0) = 0$. The EGR is similar to a flow through a restriction. In accordance to [6], we choose to model it under the form

$$g(u) \triangleq \Theta_{egr} u \tag{5}$$

where Θ_{egr} is a constant depending on the exhaust temperature, the pressure ratio between intake and exhaust manifold, and the behavior of the cooling system.

ISOTHERMAL CASE

In this part, we assume that variations of temperature in Equation (3) are small, i.e. $\dot{T} = 0$. This leads to

$$\gamma_{air} D_{air} T_{air} + \gamma_{egr} D_{egr} T_{egr} - \gamma_{int} D_{asp} T_{int} = (D_{air} + D_{egr} - D_{asp}) T_{int}$$

Further, we assume that the volumetric efficiency error is null, i.e. $\delta\eta = 0$. Moreover, we assume that with a fixed distribution, the internal recirculated gas locked in the cylinder are negligible. Under these assumption, we now present the reference model dynamics and propose an observer.

REFERENCE MODEL Let

$$x = \begin{bmatrix} P_{int} & F_{int} & \Theta_{egr} \end{bmatrix}^T \in \mathbb{R}^3$$

be the state and $y = P_{int}$ the measurement. We note $\alpha_{int} \triangleq \frac{RT_{int}}{V_{int}}$ and $\beta_{int} \triangleq \frac{1}{RT_{int}} V_{cyl} \frac{N_e}{120}$. Using (1) and (3), the reference dynamics reads

$$\begin{cases} \dot{x}_1 &= \alpha_{int} \left(D_{air} + x_3 u - \eta_{vol,map}(x_1, N_e) \beta_{int} x_1\right) \\ \dot{x}_2 &= \frac{\alpha_{int}}{x_1} \left(F_{exh} x_3 u - (D_{air} + x_3 u) x_2\right) \\ \dot{x}_3 &= 0 \\ y &= x_1 \end{cases} \tag{6}$$

Notations are summarized in Table 2.

Table 2: Variables description (isothermal observer).

Var.	Symb.
x_1	P_{int}
x_2	F_{int}
x_3	Θ_{egr}
y	P_{int}
α_{int}	$\frac{RT_{int}}{V_{int}}$
β_{int}	$\frac{1}{RT_{int}} V_{cyl} \frac{N_e}{120}$

OBSERVER DESIGN The observer dynamics are

$$\begin{cases} \dot{\hat{x}}_1 &= \alpha_{int} \left(D_{air} + \hat{x}_3 u - \eta_{vol,map}(y, N_e) \beta_{int} \hat{x}_1\right) \\ & \quad -L_1(\hat{x}_1 - y) \\ \dot{\hat{x}}_2 &= \frac{\alpha_{int}}{y} \left(F_{exh} \hat{x}_3 u - (D_{air} + \hat{x}_3 u) \hat{x}_2\right) \\ \dot{\hat{x}}_3 &= -L_3(\hat{x}_1 - y) \end{cases} \tag{7}$$

with $(L_1, L_3) \in (\mathbb{R}^+ \setminus \{0\})^2$. One can notice that (7) is a copy of (6) with additive tracking terms. Unknowns are partially substituted with output measurement. The state-error is $\tilde{x} \triangleq x - \hat{x}$. Classically, the error dynamics are

$$\begin{cases} \dot{\tilde{x}}_1 &= \alpha_{int} \left(\tilde{x}_3 u - \eta_{vol,map}(y, N_e) \beta_{int} \tilde{x}_1\right) - L_1 \tilde{x}_1 \\ \dot{\tilde{x}}_2 &= \left(F_{exh} \tilde{x}_3 u - (D_{air} + \hat{x}_3 u) \tilde{x}_2\right) \\ & \quad + \frac{\alpha_{int}}{y} (F_{exh} - x_2) \tilde{x}_3 \\ \dot{\tilde{x}}_3 &= -L_3 \tilde{x}_1 \end{cases}$$

Tuning parameters are chosen as follows

$$\begin{cases} L_1 &= (l_1 - \eta_{vol,map}(y, N_e)) \alpha_{int} \beta_{int} \\ L_3 &= l_3 \alpha_{int} u \end{cases}$$

where l_1 and l_3 are positive constants. With this choice, the error system writes under the triangular form (8)-(9)

$$\begin{cases} \dot{\tilde{x}}_1 &= \alpha_{int} \left(\tilde{x}_3 u - l_1 \beta_{int} \tilde{x}_1\right) \\ \dot{\tilde{x}}_3 &= -l_3 \alpha_{int} \tilde{x}_1 u \end{cases} \tag{8}$$

$$\dot{\tilde{x}}_2 = \frac{\alpha_{int}}{y} \left(F_{exh} \tilde{x}_3 u - (D_{air} + \hat{x}_3 u) \tilde{x}_2\right) + \frac{\alpha_{int}}{y} (F_{exh} - x_2) \tilde{x}_3 \tag{9}$$

CONVERGENCE ANALYSIS To investigate convergence of the proposed observer we restrict ourselves to the study around fixed operating point, i.e. F_{exh}, T_{int}, N_e,

and u are assumed to be constant (α_{int} and β_{int} are then constant too). Moreover, we assume that $u > 0$. This last assumption is not restrictive since u equals 0 implies that the EGR valve is completely closed and that, consequently, the EGR flow and the BGR are equal to 0.

$(\tilde{x}_1, \tilde{x}_3)$-dynamics The errors dynamics (8) is upper-triangular. Indeed, the $(\tilde{x}_1, \tilde{x}_3)$-dynamics is independent of $\tilde{x}_2$. Moreover, this dynamics is linear

$$\begin{bmatrix} \dot{\tilde{x}}_1 \\ \dot{\tilde{x}}_3 \end{bmatrix} = A_{int} \begin{bmatrix} \tilde{x}_1 \\ \tilde{x}_3 \end{bmatrix}$$

$$\text{where } A_{int} \triangleq \begin{bmatrix} -l_1\alpha_{int}\beta_{int} & \alpha_{int}u \\ l_2\alpha_{int}u & 0 \end{bmatrix}$$

A_{int} is a constant asymptotically stable matrix. This implies that $\tilde{x}_1$ and $\tilde{x}_3$ are exponentially stable, in other words $\exists(\lambda_{int}, \tau_{int,1}, \tau_{int,2}) \in (\mathbb{R} \setminus \{0\})^3$ s. t.

$$\forall t > 0, \ |\tilde{x}_1(t)| \leq \tau_{int,1} e^{-\lambda_{int} t} \text{ and } |\tilde{x}_3(t)| \leq \tau_{int,2} e^{-\lambda_{int} t}$$

$\tilde{x}_2$-dynamics On the other hand, the $\tilde{x}_2$ dynamics writes

$$\dot{\tilde{x}}_2 = -a_{int}(t)\tilde{x}_2 + b_{int}(t)\tilde{x}_3$$

where $a_{int} \triangleq \frac{\alpha_{int}}{y}(D_{\text{air}} + \hat{x}_3 u)$ and $b_{int} \triangleq \frac{\alpha_{int}}{y}(F_{\text{exh}} - x_2)u$ are bounded strictly positive parameters. For all $t \geq 0$, $0 < a_m \leq a_{int}(t) \leq a_M$ and $0 < b_m \leq b_{int}(t) \leq b_M$. Then,

$$\dot{\tilde{x}}_2 \leq -a_{int}(t)\tilde{x}_2 + b_M \tau_{int,2} e^{-\lambda_{int} t}$$

for $t > 0$. Integration leads to

$$\tilde{x}_2(t) \leq -\int_0^t a_{int}(s)\tilde{x}_2(s)ds + c_{int}^+$$

where $c_{int}^+ \triangleq \tilde{x}_2(0) + \frac{b_M \tau_{int,2}}{\lambda_{int}}$. Gronwall's Lemma (see [7]) implies

$$\tilde{x}_2(t) \leq c_{int}^+ e^{-\int_0^t a_{int}(s)ds} \leq c_{int}^+ e^{-a_m t}$$

Similarly, one can check that there exists a positive constant c_{int}^- such that $\tilde{x}_2(t) \geq -c_{int}^- e^{-a_m t}$. In summary, about a fixed operating point, the observation error is globally exponentially stable and the following result holds.

Proposition 1 *For any fixed operating point, i.e. constant values of F_{exh}, T_{int}, N_e, and $u > 0$, the state of observer* (7) *exponentially converges towards the state of system* (6)*.*

ADIABATIC CASE

In this part, we do not assume that the variation of temperature in Equation (3) is small, but rather that

$$\gamma_{air} = \gamma_{egr} = \gamma_{int} \triangleq \gamma$$

Moreover, as previously, we assume that with a fixed distribution, the internal recirculated gas locked in the cylinder are negligible. This case is of interest because for large variations of EGR, the temperature of the intake manifold can increase by 30^o during the transient (this factor actually depends on the EGR cooling system). This rules out the isothermal assumption, and generates a tracking error and a nonzero volumetric efficiency offset $\delta\eta$ in the previously presented observer. Indeed, when the EGR valve is open, one cannot distinguish an error on the EGR flow from an error on the aspirated flow (which is based on experimental *steady state* values). Yet, using an EGR temperature sensor, one can reconstruct the volumetric efficiency error $\delta\eta$ and the EGR flow. This is the subject of the following section.

REFERENCE MODEL Let

$$x = \begin{bmatrix} P_{int} & T_{int} & F_{int} & \Theta_{egr} & \delta\eta \end{bmatrix}^T \in \mathbb{R}^5$$

be the state and $y = \begin{bmatrix} P_{int}, T_{int} \end{bmatrix}^T \in \mathbb{R}^2$ the measurement. We note $\xi_{int} \triangleq \frac{R}{V_{int}}$ and $\rho_{int} \triangleq \frac{1}{R} V_{cyl} \frac{N_e}{120}$. The reference dynamics is

$$\begin{cases} \dot{x}_1 &= \xi_{int}\big(D_{air}T_{air} + x_4 u T_{egr} \\ &\quad -(\eta_{vol,map}(x_1, N_e) + x_5)\rho_{int}x_1\big) \\ \dot{x}_2 &= \frac{\xi_{int}}{x_1}\Big(D_{air}(\gamma T_{air} - x_2) + x_4 u(\gamma T_{egr} - x_2) \\ &\quad -(\gamma - 1)(\eta_{vol,map}(x_1, N_e) + x_5)\rho_{int}x_1\Big) \\ \dot{x}_3 &= \frac{\xi_{int}x_2}{x_1}\left(F_{exh}x_4 u - (D_{air} + x_4 u)x_3\right) \\ \dot{x}_4 &= 0 \\ \dot{x}_5 &= 0 \\ y &= x_1 \end{cases} \tag{10}$$

Notations for this part is summarized in Table 3.

Table 3: Variables description (adiabatic case).

Var.	Symb.
x_1	P_{int}
x_2	T_{int}
x_3	F_{int}
x_4	Θ_{egr}
x_5	$\delta\eta$
y_1	P_{int}
y_2	T_{int}
ξ_{int}	$\frac{R}{V_{int}}$
ρ_{int}	$\frac{V_{cyl}}{R}\frac{N_e}{120}$

OBSERVER DESIGN The observer dynamics are

$$\begin{cases} \dot{\hat{x}}_1 &= \xi_{int}\big(D_{air}T_{air} + \hat{x}_4 u T_{egr} \\ &\quad -(\eta_{vol,map}(y_1, N_e) + \hat{x}_5)\rho_{int}\hat{x}_1\big) \\ &\quad -L_1(\hat{x}_1 - y_1) \\ \dot{\hat{x}}_2 &= \frac{\xi_{int}}{y_1}\big(D_{air}(\gamma T_{air} - \hat{x}_2) + \hat{x}_4 u(\gamma T_{egr} - \hat{x}_2) \\ &\quad -(\gamma - 1)(\eta_{vol,map}(y_1, N_e) + \hat{x}_5)\rho_{int}y_1\big) \\ &\quad -L_2(\hat{x}_2 - y_2) \\ \dot{\hat{x}}_3 &= \frac{\xi_{int}y_2}{y_1}\left(F_{exh}\hat{x}_4 u - (D_{air} + \hat{x}_4 u)\hat{x}_3\right) \\ \dot{\hat{x}}_4 &= -L_{4,1}(\hat{x}_1 - y_1) - L_{4,2}(\hat{x}_2 - y_2) \\ \dot{\hat{x}}_5 &= L_{5,1}(\hat{x}_1 - y_1) + L_{5,2}(\hat{x}_2 - y_2) \end{cases} \tag{11}$$

with $(L_1, L_2, L_4, L_5) \in (\mathbb{R}^+ \setminus \{0\})^4$. Again, one can notice that (11) is a copy of (10) with additive tracking terms and where unknowns are partially substituted with output measurements. The state-error is $\tilde{x} \triangleq x - \hat{x}$. Classically, the error dynamics is

$$\left\{\begin{array}{rcl} \dot{\tilde{x}}_1 &=& \xi_{int}\big(\tilde{x}_4 u T_{egr} - \eta_{vol,map}(y_1, N_e)\rho_{int}\tilde{x}_1 \\ && \quad -\rho_{int}(x_5\tilde{x}_1 + \hat{x}_1\tilde{x}_5)\big) \\ && \quad -L_1\tilde{x}_1 \\ \dot{\tilde{x}}_2 &=& \frac{\xi_{int}}{y_1}\big(-D_{air}\tilde{x}_2 + \tilde{x}_4 u(\gamma T_{egr} - \hat{x}_2) \\ && \quad -u x_4\tilde{x}_2 - (\gamma-1)\tilde{x}_5\rho_{int}y_1\big) \\ && \quad -L_2\tilde{x}_2 \\ \dot{\tilde{x}}_3 &=& \frac{\xi_{int}y_2}{y_1}\left(-(D_{air} + u\hat{x}_4)\tilde{x}_3 + (F_{exh} - u x_3)\tilde{x}_4\right) \\ \dot{\tilde{x}}_4 &=& -L_{4,1}\tilde{x}_1 - L_{4,2}\tilde{x}_2 \\ \dot{\tilde{x}}_5 &=& L_{5,1}\tilde{x}_1 + L_{5,2}\tilde{x}_2 \end{array}\right.$$

Tuning parameters are chosen as follows

$$\left\{\begin{array}{rcl} L_1 &=& (l_1 - \eta_{vol,map}(y, N_e))\xi_{int}\rho_{int} \\ L_2 &=& l_2\frac{\xi_{int}}{y_1}D_{air} \\ L_{4,1} &=& l_4\xi_{int}T_{egr}u \\ L_{4,2} &=& l_4\frac{\xi_{int}}{y_1}u(\gamma T_{egr} - \hat{x}_2) \\ L_{5,1} &=& l_5\xi_{int}\rho_{int}\hat{x}_1 \\ L_{5,2} &=& l_5\frac{\xi_{int}}{y_1}(\gamma-1)\rho_{int}y_1 \end{array}\right.$$

With this choice, the error system writes under the following triangular form

$$\left\{\begin{array}{rcl} \dot{\tilde{x}}_1 &=& \xi_{int}\big(\tilde{x}_4 u T_{egr} - l_1\rho_{int}\tilde{x}_1 \\ && \quad -\rho_{int}(x_5\tilde{x}_1 + \hat{x}_1\tilde{x}_5)\big) \\ \dot{\tilde{x}}_2 &=& \frac{\xi_{int}}{y_1}\big(-(1+l_2)D_{air}\tilde{x}_2 + \tilde{x}_4 u(\gamma T_{egr} - \hat{x}_2) \\ && \quad -u x_4\tilde{x}_2 - (\gamma-1)\tilde{x}_5\rho_{int}y_1\big) \\ \dot{\tilde{x}}_4 &=& -l_4\xi_{int}T_{egr}u\tilde{x}_1 \\ && \quad -l_4\frac{\xi_{int}}{y_1}u(\gamma T_{egr} - \hat{x}_2)\tilde{x}_2 \\ \dot{\tilde{x}}_5 &=& l_5\xi_{int}\rho_{int}\hat{x}_1\tilde{x}_1 \\ && +l_5\frac{\xi_{int}}{y_1}(\gamma-1)\rho_{int}y_1\tilde{x}_2 \end{array}\right. \quad (12)$$

$$\dot{\tilde{x}}_3 = \frac{\xi_{int}y_2}{y_1}\left(-(D_{air} + u\hat{x}_4)\tilde{x}_3 + (F_{exh} - u x_3)\tilde{x}_4\right) \quad (13)$$

OBSERVER CONVERGENCE

Lyapunov function candidate Convergence of (12) towards $\{0\}$ can be proven through a Lyapunov stability analysis. A Lyapunov function candidate is

$$V(\tilde{x}) = \frac{1}{\xi_{int}}\left(\tilde{x}_1^2 + \tilde{x}_2^2 + \frac{1}{l_4}\tilde{x}_4^2 + \frac{1}{l_5}\tilde{x}_5^2\right) \quad (14)$$

Differentiation yields

$$\begin{array}{rcl} \dot{V}(\tilde{x}) &=& \frac{1}{\alpha_{int}}(\tilde{x}_1\dot{\tilde{x}}_1 + \frac{1}{\alpha_{int}}\tilde{x}_2\dot{\tilde{x}}_2 \\ && +\frac{1}{\alpha_{int}l_4}\tilde{x}_4\dot{\tilde{x}}_4 + \frac{1}{\alpha_{int}l_5}\tilde{x}_5\dot{\tilde{x}}_4) \\ &=& -l_1\rho_{int}\tilde{x}_1^2 \\ && -\frac{1}{y_1}\left((1+l_2)D_{air} + u x_4\right)\tilde{x}_2^2 \end{array}$$

Thus, $V(0) = 0$, and $\forall \tilde{x} \in \mathbb{R}^2\setminus\{0\}\ V(\tilde{x}) > 0$ and $\dot{V}(\tilde{x}) \leq 0$. The next lemma holds

Lemma 1 *The function V defined by* (14) *is a Lyapunov function for the error-state system* (12)*.*

Application of LaSalle's theorem Let $\Omega_r = \{\tilde{x}_f \in \mathbb{R}^4 / V(\tilde{x}_f) < r\} \subset \mathbb{R}^4$. It is a compact set positively invariant with respect to the error dynamics (12) because $\dot{V} \leq 0$. In summary, V is a continuously differentiable function such that $\dot{V}(\tilde{x}_f) \leq 0$ in Ω_r. Let I_f be the largest invariant set in $\{\tilde{x}_f \in \Omega_r / \dot{V}(\tilde{x}_f) = 0\}$. From LaSalle's theorem (see [7] Theorem 4.4), every solution starting in Ω_r approaches I_f as $\alpha \to \infty$.

Characterization of the invariant set I_f We first characterize $\{\tilde{x}_f \in \Omega_r / \dot{V}(\tilde{x}_f) = 0\}$ and then I_f. First,

$$\tilde{x}_f \in \{\tilde{x}_f \in \Omega_r / \dot{V}(\tilde{x}_f) = 0\} \Leftrightarrow \left\{\begin{array}{l} \tilde{x}_{1_f} = 0 \\ \tilde{x}_{2_f} = 0 \end{array}\right.$$

because η_{vol} and β_{int} are positively bounded. Thus from LaSalle's theorem, I_f is the largest invariant set in $\{\tilde{x}_f \in \Omega_r / \dot{V}(\tilde{x}_f) = 0\}$. It writes

$$I_f = \left\{ \left[\begin{array}{cccc} 0 & 0 & \tilde{x}_{4,f} & \tilde{x}_{5,f} \end{array}\right]^T \in \mathbb{R}^2 / \mathcal{L}_{int} \left[\begin{array}{c} \tilde{x}_{4,f} \\ \tilde{x}_{5,f} \end{array}\right] = 0 \right\}$$

where

$$\mathcal{L}_{int} \triangleq \left[\begin{array}{cc} \xi_{int}T_{egr}u & \frac{\xi_{int}}{y_1}u(\gamma T_{egr} - x_2) \\ \xi_{int}\rho_{int}x_1 & \frac{\xi_{int}}{y_1}(\gamma-1)\rho_{int}y_1 \end{array}\right]$$

$$\det(\mathcal{L}_{int}) = -\xi_{int}^2\rho_{int}u(T_{egr} - T_{int})$$

Yet, the intake temperature never equals the EGR temperature (there are at least a 10 difference). When the valve is open, the set I_f is reduced to $\{0\}$. Then, $\{0\}$ is asymptotically stable for the error dynamics (12) and the following result holds.

Lemma 2 *If $u > 0$ (EGR valve open), then the largest set in*

$$\Omega_r = \{\tilde{x}_f \in \mathbb{R}^2 / V(\tilde{x}_f) < r\} \subset \mathbb{R}^2$$

invariant by the dynamics (12) *is the null space.*

Convergence proof of $\tilde{x}_3$ is similar to the technique presented in the previous section.

In summary, about a fixed operating point, the observation error is asymptotically stable and the following result holds.

Proposition 2 *For any fixed operating point, i.e. constant values of F_{exh}, T_{int}, N_e, and $u > 0$, the state of observer* (11) *asymptotically converges towards the state of system* (10)*.*

SIMULATOR

IFP-ENGINE LIBRARY The engine system simulation tool used for this study is the IFP-ENGINE library. It has been developed in the IMAGINE's numerical platform AMESim which is an environment for modelling and simulating dynamical systems (using a Bond Graph approach).

Gas under consideration consist of 3 species : fresh air, vaporized fuel and burned gas. Two efficient phenomenological models are available for gasoline [8] and Diesel combustion [9].

HPC DIESEL ENGINE MODEL The model under consideration runs 20 times slower than real time (with a variable time step solver on a 3 GHz PC). Air path includes a compressor, pipes, a heat exchanger, a throttle and an intake manifold. All these elements are represented by dedicated submodels. The compromise to be done between the engine model accuracy and the simulation time cost has a major impact on the complexity of the phenomena taken into account in this part of the engine model. High frequency pulses modelling in the intake manifold can be heavily time consuming. A reasonable compromise between accuracy of instantaneous pressure fluctuations and time consumption must be made. This is done by comparing different levels of manifold modelling details. For our purpose, the best compromise is the approach yielding the lowest time consumption while limiting the effect of in-manifold phenomena neglection on neighboring elements. The combustion chamber is connected to the air path through the cylinder head which acts thanks to valve lift laws and permeability behavior model derived from experimental characterization. The fuel injection system allows to perform up to three injections per cycle that are controlled with the common rail pressure by means of injection starting time and duration. Cylinder wall heat losses are modelled using a Woschni's approach with three independent temperature variables for the cylinder head, the piston and the liner. The combustion heat release model is based on a conventional 0D Diesel combustion model approaches [10, 11] extended to multi-pulse injection, auto-ignition delay and EGR effect correction in order to get good combustion behavior in the whole range of operating set points, especially in both Highly Premixed Combustion (HPC) and conventional combustion modes. A typical result is reported in Figure 3 (see [12] for more details). The air path of the engine is equipped with an air throttle, an EGR valve and a Variable Geometry Turbocharger. This model is a good representation of the main phenomena of the engine and is an appropriate tool for control purposes.

SIMULATION RESULTS

IMEP TRAJECTORY We test our observer on a transient 4-10-4 bar of IMEP at 1500 rpm. The trajectories of the EGR valve and the BGR are reported in Figure 4. The trajectories of the EGR flow rate and intake pressure are reported in Figure 5.

OBSERVERS RESULTS We focus on 3 time zones of the observers responses.

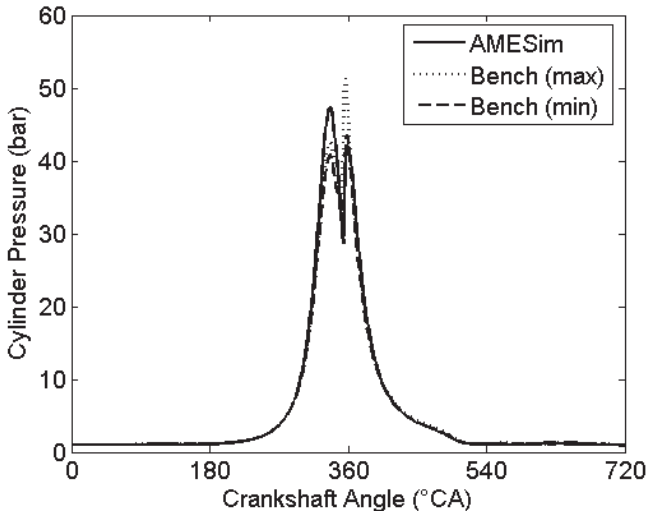

Figure 3: Model/Test bench cylinder pressure comparison at IMEP = 6 bar (EGR = 35 %).

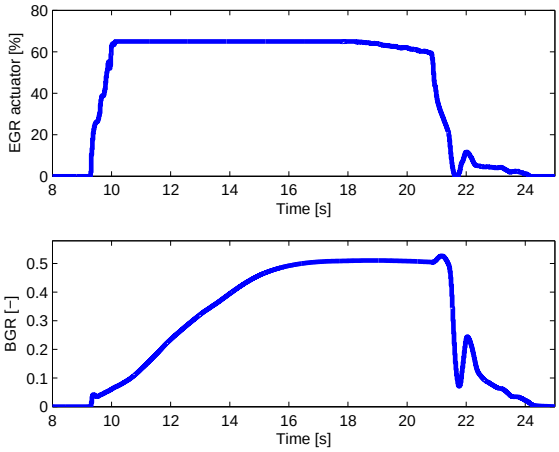

Figure 4: Transient at 1500 rpm, IMEP: $10 - 4 - 10$ bar. Top: EGR actuator, bottom: BGR.

- Time zone 1 : $[9,\ 12.5]$ the EGR valve opens (Figure 6). Both observers have relevant slopes. Interestingly, the adiabatic observers catches the overshoot at the beginning.
- Time zone 2 : $[15,\ 20]$ the EGR flow stabilizes (Figure 7). The adiabatic converges towards the reference BGR while the isothermal observer has a volumetric efficiency error $\delta\eta$ yielding an offset error in the BGR tracking.
- Time zone 3 : $[21,\ 25]$ the EGR valve closes with one oscillation (Figure 8). Both observers have the same dynamic, they follow the BGR dynamics during the oscillation of the EGR valve.

Simulation results stress the relevance of the proposed observers. Both seems appropriate for control purposes. The dynamical behavior of the system is well captured. Further, the adiabatic observer provides an estimation of the volumetric efficiency. This gives the exact total quan-

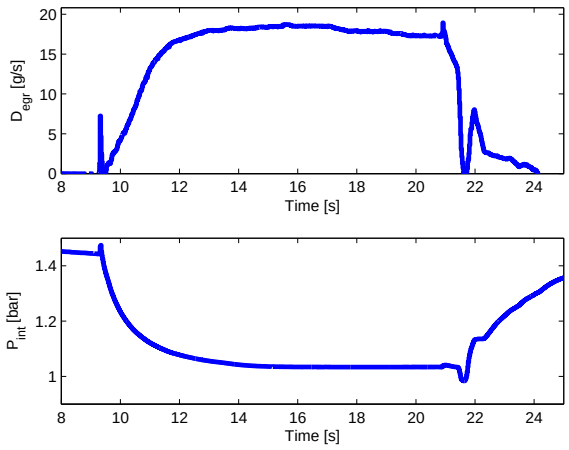

Figure 5: Transient at 1500 rpm, IMEP: $10-4-10$ bar. Top: EGR flow (g.s^{-1}), bottom: intake pressure (bar).

tity of air aspirated into the cylinders. In that case, an accurate EGR and aspirated flows observation is done with two extra temperature sensors (fresh air and EGR temperatures). The static error on aspirated flow is eliminated and leads to convergence of both the EGR flow and the BGR.

ERROR SENSITIVITY We proved that systems (6) and (10) are observable for any fixed operating conditions, i.e. constant values of F_{exh}, T_{int}, N_e, and an opened EGR valve ($u > 0$). First, the assumption $\frac{dT}{dt}$ equals 0 is not restrictive for the convergence of the observer because the temperature dynamics is stable. Moreover, yet, when the EGR valve is closed, one cannot estimate Θ_{egr}. This variable depends on the exhaust temperature, the pressure ratio between intake and exhaust manifold, and the behavior of the cooling system. Results for different initial increasing initial value of $\hat{\Theta}_{egr}$ with the isothermal observer are presented in Figure 9. The beginning of the transient part depends on the initial condition on $\hat{\Theta}_{egr}$. Changing the operating point without opening the EGR valve will have an influence on Θ_{egr}. More precisely, increasing the load increases Θ_{egr}. A next step is to estimate Θ_{egr} when the EGR valve is closed. This would yield a faster estimation of the BGR when the EGR valve opens. We are currently investigating that point.

CONCLUSION AND FUTURE DIRECTIONS

This paper presents two observers for the estimation of the burned gas ratio in the air path dynamics. After presenting the model in Section 2, two observers are derived based on different assumptions (in Section 3 and in Section 4). Simulations results are reported in Section 6. These show that the use of the EGR temperature sensor yields convergence of the aspirated flow estimation. This precisely characterizes the amount of air and BGR aspirated by the cylinder. The observers performances are summarized in Table 4.

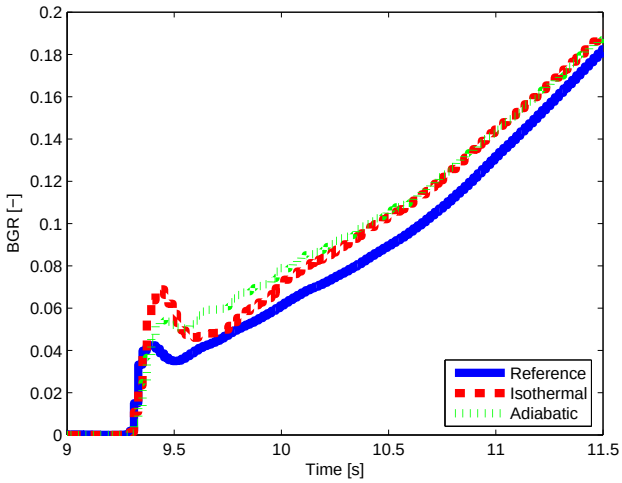

Figure 6: Observer results on a transient at 1500 rpm, IMEP from 10 to 4 bar, EGR valve is opening. Blue: reference, red-dashed: isothermal observer, green-dotted: adiabatic observer. Both observers feature consistant slopes. The adiabatic observer catches the overshoot at the beginning.

Table 4: Summary.

	Isothermal	**Adiabatic**
Sensors:		
P_{int}	Needed	Needed
T_{int}	Needed	Needed
D_{air}	Needed	Needed
AFR	Needed	Needed
T_{air}	Not Needed	Needed
T_{egr}	Not Needed	Needed
Volumetric efficiency:		
$\delta\eta$	0 by assumption	Estimated
D_{egr} estimation:		
	Offset due to $\delta\eta$	Convergence
BGR estimation:		
	Offset due to $\delta\eta$	Convergence

References

[1] J. Kahrstedt, K. Behnk, A. Sommer, and T. Wormbs. Combustion processes to meet future emission standards. In *Motortechnische Zeitschrift*, pages 1417–1423, 2003.

[2] A. Hultqvist, U. Engdar, B. Johansson, and J. Klingmann. Reacting boundary layers in a homogeneous charge compression ignition (HCCI) engine. In *Proc. of SAE Conference*, number 2001-01-1032, 2001.

[3] B. Walter and B. Gatellier. Development of the high power NADI^{TM} concept using dual mode Diesel combustion to achieve zero NOx and particulate emissions. In *Proc. of SAE Conference*, number 2002-01-1744, 2002.

[4] S. Bittanti, P. Colaneri, and G. De Nicolao. Application of input estimation techniques to charge es-

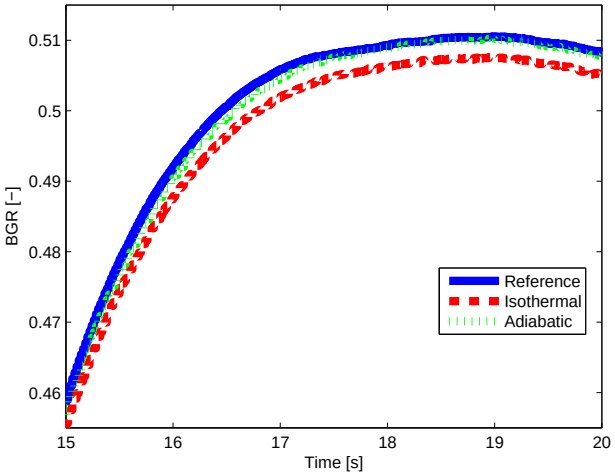

Figure 7: Observer results on a transient at 1500 rpm, IMEP from 10 to 4 bar, EGR is settling . Blue: reference, red-dashed: isothermal observer, green-dotted: adiabatic observer. The adiabatic observer converges towards the reference BGR contrary to the isothermal observer that suffers from a non-zero volumetric efficiency error $\delta\eta$.

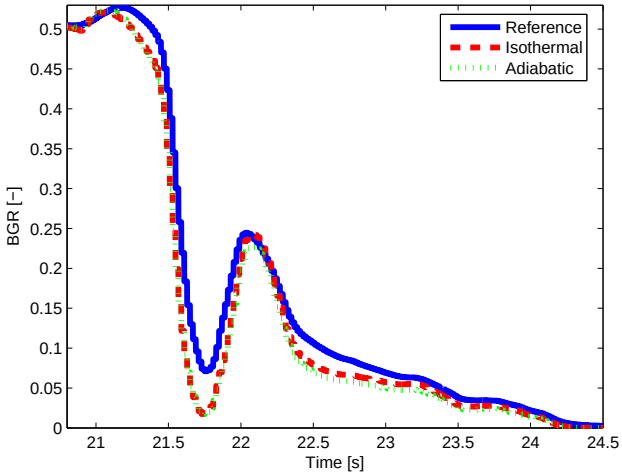

Figure 8: Observer results on a fast transient at 1500 rpm, IMEP from 4 to 10 bar, EGR valve is closing with an oscillation. Blue: reference, red-dashed: isothermal observer, green-dotted: adiabatic observer. Both observers have the same dynamic, they follow the BGR dynamics during the oscillation of the EGR valve.

timation and control in automotive engines. *Control Engineering Practice*, 10:1371–1383, 2002.

[5] M. Müller, P. Olin, and B. Schreurs. Dynamic EGR estimation for production engine control. In *Proc. of SAE Conference*, number 2001-01-05533, 2001.

[6] J. Heywood. *Internal Combustion Engine Fundamentals*. McGraw-Hill, Inc, 1988.

[7] H. Khalil. *Nonlinear Systems*. Prentice-Hall, Inc., 1992.

[8] F. Lafossas, O. Colin, F. Le Berr, and P. Ménégazzi. Application of a new 1d combustion model to gasoline transient engine operation. In *Proc. of SAE Conference*, number 2005-01-2107, 2005.

[9] T. Jaine, A. Benkenida, P. Ménégazzi, and P. Higelin. Zero dimensional computation of diesel spray - comparison with experiments and 3d model. In *6^{th} International Conference on Engines for Automobile, Capri, Italy*, 2003.

[10] F. Chmela and G. Orthaber. Rate of heat release prediction for direct injection Diesel engines based on purely mixing controlled combustion. In *Proc. of SAE Conference*, number 1999-01-0186, 1999.

[11] C. Barba and C. Burkhardt. A phenomenological combustion model for heat release rate prediction in high-speed DI Diesel engines with common rail injection. In *Proc. of SAE Conference*, number 2000-01-2933, 2000.

[12] A. Albrecht, J. Chauvin, S. Potteau, and G. Corde. Design of real-time torque balancing control for highly premixed combustion engine using a 1d Diesel engine model. In *Proc. of the IAV Conference "Engine process simulation and supercharging"*, 2005.

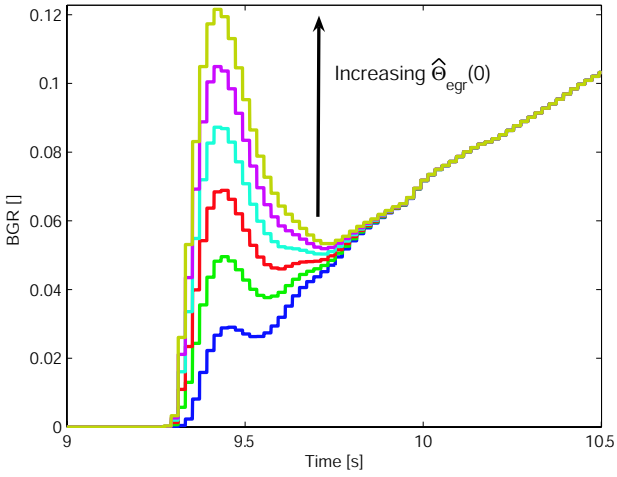

Figure 9: Isothermal observer results on a fast transient at 1500 rpm, IMEP from 10 to 4 bar, with increasing initial value of $\hat{\Theta}_{egr}$. $\hat{\Theta}_{egr}(0)$ from 0 to 50.